Turkish Computational and Theoretical Chemistry

Turkish Comp Theo Chem (TC&TC)

Volume(Issue): 8(1) – Year: 2024 – Pages: 65-79

e-ISSN: 2602-3237

https://doi.org/10.33435/tcandtc.1252038

Received: 12.02.2023 ***Accepted:*** 27.04.2023 *Research Article*

Theoretical insights on the relationship between detection limit and complex stability of oxine ligand

Boulanouar MESSAOUDI[a,b,1], Naceur BENHADRIA[a], Tarik ATTAR[a,b]

[a] Ecole Supérieure en Sciences Appliquées de Tlemcen, ESSA-Tlemcen, BP 165 RP Bel Horizon, Tlemcen 13000, Algeria

[b]Laboratory of ToxicoMed, University of Abou Bekr Belkaïd, B.P.119, Tlemcen, 13000, Algeria

Abstract: The concept of detection limit was combined with quantum chemical calculations for trace analysis of cadmium and lead in aqueous solution using deprotonated 8-hydroxyquinoline (oxine) as ligand. The DFT study was performed using 6-31G(d), cc-pVTZ and SDD basis sets in combination with different theoretical methods such as; B3LYP, MP2 and M06L implemented in Gaussian 09 program package. The obtained results of the study in the gas and aqueous phases show that the chemical stability of the complex was found in the order Pb-oxine > Cd-oxine. Based on the calculations done, the stability order was relative to the detection limit (LOD) for the two metals Cd and Pb. Thus, a reverse relationship between LOD and binding energy has been found.

Keywords: Cadmium, Lead, Oxine, Binding energy, DFT.

1. Introduction

Pollution by heavy metals is mostly a result of mining and smelting in industrial processes, as well as the use of metal compounds in households and agriculture. Among this type of pollution, lead and cadmium are toxic elements for the human organism. The two elements can be very dangerous even at low concentrations [1]. The main sources of exposure to lead and cadmium are industrial and automobile exhaust, water from lead pipes, paints, lead-containing cans, ceramics, plastics, battery manufacturing, alloys, smelting, refining, and printing [2]. The ionic mechanism of Pb toxicity occurs principally due to the capacity of lead metal ions to replace other bivalent cations like calcium, magnesium, iron and monovalent cations like sodium, which ultimately disturbs the biological metabolism of the cell [3, 4]. Moreover, the cadmium ion crosses the cell membrane through calcium channels, especially when extracellular calcium levels are low [5]. Serious disorders can be caused by high level of lead ions, such as nausea, convulsions, coma, renal failure, cancer, and subtle effects on the metabolism and intelligence. On the other hand, an excess of Cd in the human body may cause erythrocyte destruction, nausea, salivation, diarrhea, muscular cramps, renal degradation, and chronic pulmonary problems [6]. Electrochemical methods offer many advantages compared to spectrometric and chromatographic methods, since the equipments are less expensive, faster, and easier to be operated and the measurements can be carried out directly on site [7]. In addition, the other methods analyze the total concentration of metal, while electroanalytical techniques allow analysis of metals under different oxidation numbers. The use of electroanalytical techniques is of a considerable importance due to their high degree of sensitivity, accuracy, and selectivity as well as large linear dynamic range; they even have low detection and determination limits [8, 9].A detection limit (LOD) is an essential parameter in analytical methods,

[1] Corresponding Authors

e-mail: messaoudiboulanouar@gmail.com

which is defined as the lowest quantity or concentration of an analyte in a sample that can be reliably detected with a given analytical method, but not necessarily quantified with an acceptable uncertainly [10]. LOD was calculated from the equations in which the standard deviation of response and the slope of the calibration curve were used. The adsorptive stripping voltammetric (AdSV) is based on current measurement as a function of voltage and it is followed by the reduction of the metal complex adsorbed on the surface of the working electrode by providing a reduction potential rapidly [11, 12]. These techniques are powerful analytical tools that are becoming widely used in various analysis fields such as: trace essential elements, toxic metals, food additive dyes, pesticide, fertilizers and veterinary drugs residuals, other organic compounds of biological and other compounds. The adsorptive stripping voltammetry (AdSV) has been shown to be an efficient technique for assay of trace amount of a wide range of species, which have interfacial adsorptive character onto the working electrode surface [13]. The technique is strongly influenced by the following variables: the concentration and nature of the complexing agent, pH, potential accumulation, and time accumulation. The choice of ligands is the most important component in the AdSV method because of the selectivity, sensitivity, and accuracy of the method are determined by the complex used. As previously mentioned, metal imbalance is the leading cause for numerous diseases, thus, 8-hydroxyquinoline is a strong complexing agent that may re-establish metal balance and be helpful for the treatment of metal-related diseases. 8-hydroxyquinoline, also known as oxine or 8-quinolinol, has an effective coordinating ability and good metal recognition properties, which means that it is extensively used for analytical and separation purposes as well as for metal chelation such as Fe, Cu, Zn, Mn, Hg, Cd and Pb [14-20].

The oxine molecule has been widely studied experimentally and theoretically. For instance, H. Darougari and M. Rezaei-Sameti used the density functional theory (DFT) and time-dependent density functional theory (TD-DFT) at ωB97XD/Lanl2DZ level of theory to study in details the effects of Cu and Ni decorated on Boron nitride nanocage (B12N12) on the interaction of 8-hydroxyquinoline (8-HQ) drug. On the basis of thermodynamic results, they have found that the adsorption energy of 8-HQ drug with B12N12 and Cu & B12N12, Ni & B12N12 nanocages were all exothermic. The calculated gap energy and global hardness values of the Ni and Cu decorated B12N12 nanocage found to be smaller than the pristine B12N12 nanocage indicating that nanocage in this state were more conductive and reactive. They have also confirmed the partially covalent/electrostatic bond between 8-HQ drugs and B12N12 nanocage using different approaches such as: atom in molecule (AIM), reduced density gradient plots (RDG), and electron localized function (ELF) [21].

Cipurković et al. synthesized three metal complexes with square planar and octahedral geometry with 8-hydroxyquinoline (8-HQ), performed their spectral analysis and their antimicrobial effect in vitro. They have used conductometry and spectrophotometry techniques in order to determine the stoichiometric ratio of the complex and the FTIR and UV/VIS spectroscopy to characterize their structures. The antimicrobial activity has been also examined by diffusion technique. Their obtained results revealed that both oxygen and nitrogen atoms of 8-HQ are involved in the formation of the complex and that the antimicrobial activity of the complexes is high [22].

V.V.N. Ravi Kishore et al. have investigated the optical absorption and/or excitation spectrum of tris(8-hydroxyquinolinato) aluminium(III) (Alq3) in thin solid film. The spectrum of Alq3 shows two weak butprominentbands at 334 and 320 nm. These latter have been assigned to a vibronic progression due to thering deformation modes at 1300 cm-1. This assignment has beenbased on the one-to-one correspondence of the absorption bands of Alq3 and the ligand, 8-hydroxyquinoline in its protonated form. The long wavelength absorption band of Alq3 at 390 nm has been explained as a superposition of two or more electronic transitions [23].

Renaud Rahier et al. have presented the development of a direct, specific, and continuous phospholipase D assay based on the chelation-enhanced fluorescence property of 8-hydroxyquinoline. Hence, this assay is well adapted for studying the phospholipase D, and found to be effective in monitoring the competitive inhibition

of phosphatidic acid formation in the production of phosphatidylalcohols [24].

Juan Murgich and Héctor J. Franco probed theoretically the electronic charge distribution ρ(r) of the metal atoms in Mn(III), Fe(III), and Co(III) complexes of 8-hydroxyquinoline (8HQ) using the quantum theory of atoms in molecules. Their work showed the presence of eight non bonded concentrations in their valence shell. The O− and N−metal bonds were dative bonds of close shell type with a degree of covalency and the most changes in ρ(r) were located around the N and O atoms of 8HQ. They have also found that the coordination increased the aromaticity of most of the studied compounds [25].

Mario Amati et al. have performed a spectroscopic and computational investigation in order to determine the form of 8-hydroxyquinoline in different solvents. They have assigned UV−VIS, fluorescence, and IR spectral features by ab initio calculations based on the density functional theory and MP2.They have studied the relative stability of the dimeric and monomeric cis and trans forms of 8-hydroxyquinoline in various solvents. Their results showed that 8-hydroxyquinoline, as dimer or monomer, preferred the cis conformation, and that just a small fraction of the trans conformation was present in water solutions [26].

There were only four previous works published by our group that showed the relationship between the limit of detection and the energy of stability by theoretical DFT calculations by the use of a single metal with different ligands [27-30]. To confirm and elucidate the relationship between the stability of the complex and the limit of detection in electroanalysis which can provide additional information to the research scientist with a new prediction method and can be considered as a complementary to experimental result, we will study and compare the stability energy of the complex of 8-Hydroxyquinoline ligand with two metals; lead and cadmium.

The complexation chemical reaction can be given as [30]:

$$2.Ox^{-} + M^{2+} \rightleftharpoons M(Ox)_2$$

where M is Cd or Pb, and Ox– is the deprotonated oxine.

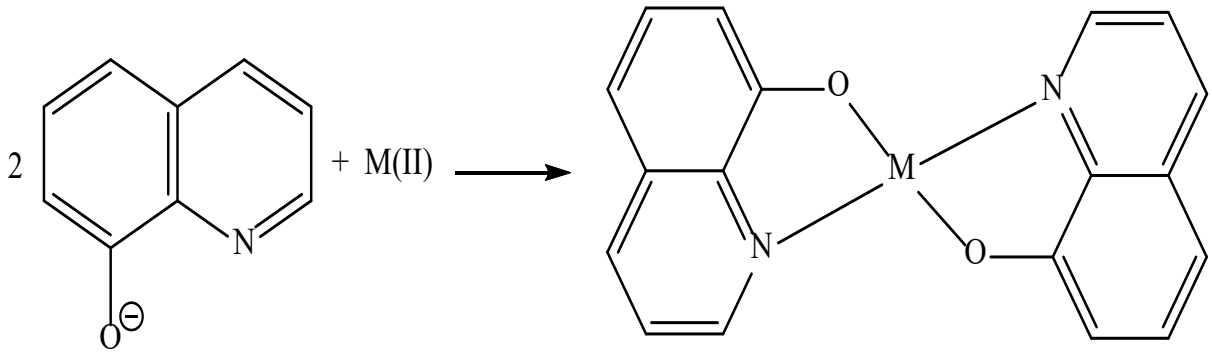

Figure 1. Complexing reaction between metal (M) and deprotonated oxine (Ox^{-}).

2. Computational Method

The theoretical calculations have been performed at B3LYP/6-31G(d), B3LYP/cc-pVTZ, MP2/6-31G(d) and M06L/6-31G(d)for H, C, O and N atoms and B3LYP/SDD, MP2/SDD and M06L/SDD for Cd and Pb atoms [31]. They were used to study the stability energy of some organic molecules and their complexes with transition metal ions [32]. Gaussian 09 program package was used for this purpose. The polarizable continuum model PCM [33-35] was used as a reaction field model of the solvation effect for the surrounding water molecules of the solvent model at a solvent dielectric constant of 78.39. The quantum calculations using density functional theory (DFT) are very successful in terms of relating the electronic density to energy. At the same level of theory, the full geometry optimizations combined with frequency calculations were performed for all the stationary points. The frequency analysis for the studied compounds demonstrated the absence of any possible imaginary frequency. The finite difference approximation (FDA) was used to calculate Fukui indices. While calculating the local indices, the geometry of the neutral system was kept for cationic and anionic systems. The

electronic populations were computed using NPA (natural population analysis) [36]. Within the standpoint of conceptual density functional theory (DFT), the electronegativity χ and hardness η are given respectively, by the equations (1) and (2) [37].

$$\chi = -\mu = -\left(\frac{\partial E}{\partial N}\right)_{\upsilon(r)} \quad (1)$$

$$\eta = \left(\frac{\partial^2 E}{\partial N^2}\right)_{\upsilon(r)} = \left(\frac{\partial \mu}{\partial N}\right)_{\upsilon(r)} \quad (2)$$

where μ is the chemical potential, N is the number of electrons, E is the total energy and υ(r) is the external potential [38].

χ and η can be expressed by using electron affinity (A) and ionization potential (I) [39]:

$$\chi = \frac{1}{2}(I + A) \quad (3)$$

$$\eta = \frac{1}{2}(I - A) \quad (4)$$

The highest occupied (HOMO) and lowest unoccupied molecular orbitals (LUMO) are related to the ionization potential and electron affinity by the following relations [40]:

$$A = -E_{LUMO} \quad (5)$$

$$I = -E_{HOMO} \quad (6)$$

Hence, χ and η can be written as [41]:

$$\chi = -\frac{1}{2}(E_{LUMO} + E_{HOMO}) \quad (7)$$

$$\eta = \frac{1}{2}(E_{LUMO} - E_{HOMO}) \quad (8)$$

The electrophilic power of a given system is characterized by the electrophilicity index ω [29]:

$$\omega = \frac{\mu}{2\eta} \quad (9)$$

The nucleophilicity (N) of a molecule is defined as the negative value of the gas phase ionization potential *IP* [27]:

$$N = -IP \quad (10)$$

Nucleophilicity defined by Domingo's group by another useful expression [42]:

$$N = E_{HOMO(Nu)} - E_{HOMO(TCE)} \quad (11)$$

Where $E_{HOMO(TCE)}$ is the highest occupied molecular orbital energy of tetracyanoethylene (TCE) taken as reference since it presents the lowest HOMO energy.

The reactivity of each site in a molecule toward a given attack is described by local quantities. For instance, Fukui function is defined as [28]:

$$f(r) = \left[\frac{\partial \rho(r)}{\partial N}\right]_{\upsilon(r)} = \left[\frac{\delta \mu}{\delta \upsilon(r)}\right]_N \quad (12)$$

where $\rho(r)$ is the electronic density of a system, N is the number of electrons and $\upsilon(r)$ is a constant external potential.

Yang and Mortier introduced the condensed form of the Fukui function as [28]:

In the case of a nucleophilic attack

$$f_k^+ = \left[\rho_k(N+1) - \rho_k(N)\right] \quad (13a)$$

while for an electrophilic attack

$$f_k^- = \left[\rho_k(N) - \rho_k(N-1)\right] \quad (13b)$$

where $\rho_k(N)$, $\rho_k(N-1)$ and $\rho_k(N+1)$ are the gross electronic populations of the site k in neutral, cationic, and anionic systems, respectively.

The population analysis (Mulliken, natural, electrostatic, *etc*.) can be used to calculate the charges. The latter equations have been applied to a variety of systems in order to look for reactivity trends. Binding energy in another quantity to be considered whenever dealing with the study of a given complex. It is basically the difference in energy between the complex and its components; the metal ion and the ligand. It is a very useful way to discuss and determine the stability of complexes and say whether one complex is more likely to be formed with respect to another [43]. On the basis of the equation (14):

$$E_b = E_{complex} - (E_{ligand} + E_{metal\ ion}) \quad (14)$$

where $E_{complex}$, E_{ligand} and $E_{metal\ ion}$, represent the energy of complex, ligands, and metal ion, respectively.

The other thermodynamic parameters such as the change in enthalpy (ΔH), and entropy (ΔS), of complexation were calculated according to the following equation:

$$\Delta H_r = \Delta H_{complex} - (\Delta H_{ligand} + \Delta H_{metalion}) \quad (15)$$

$$\Delta S_r = \Delta S_{complex} - (\Delta S_{ligand} + \Delta S_{metalion}) \quad (16)$$

Where H_i, and S_i are the enthalpy and entropy of the corresponding species, respectively.

The binding energy was calculated theoretically using the formulae [44,45]:

$$\Delta G_b = \Delta G_{complex} - (\Delta G_{ligand} + \Delta G_{metal\ ion}) \quad (17)$$

where; ΔG_b is the free energy of binding, and $\Delta G_{Complex}$, ΔG_{Ligand}, $\Delta G_{metal\ ion}$ are the energies of the metal/ligand complex, the free ligand and the free metal ion, respectively.

3. Results and discussion

The oxine molecule is of particular interest since it contains oxygen and nitrogen atoms as source of high electronic density. The complexation phenomenon on the metal surface is closely related to this heteroatom. The main goal of this research work is to show the metal effect on the complexation mechanism in terms of stability of the formed complexes and find a possible relationship with the detection limit. The optimized structure of the deprotonated oxine is given in Figure 2.a. In order to get more insight on the local reactivity, we have calculated the Fukui indices f_k^- using the numbering shown in Figure 2.b. The obtained results are presented in Table 1. The Fukui indices, f_k^-, corresponding to electrophilic attack are calculated using one type of population analysis: the natural population analysis (NPA) in order to put in evidence, the most reactive sites.

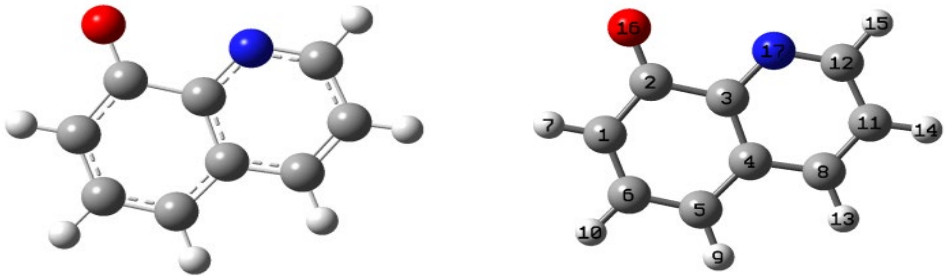

(a) (b)

Figure 2. Molecular structure (a) and numbering system of atoms of Ox^- (b).

As can be seen from Table 1, the oxygen atom has the highest local nucleophilicity index (N_k) and can be considered the most reactive site. The nitrogen atom is also a less reactive site than the oxygen, but can also contribute to the stability of the complex. In this molecule, C1 and C5 have significant N_k values but are unable to chelate with the metal atom due to steric hindrance. As a result, the oxygen and nitrogen atom centres have a greater ability to bind to the metal surface. The distribution of electron density of the frontier molecular orbitals of the molecule is another important factor to consider when studying reactions.

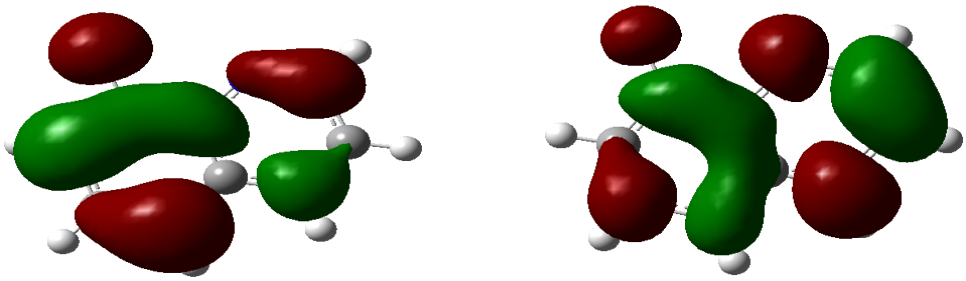

HOMO LUMO

Figure 3. Calculated HOMO and LUMO molecular orbitals of the studied molecule at the B3LYP/6-31G(d) level of theory.

The HOMO density distribution (Figure 3) is clearly scattered and bulky in the area containing the reactive oxygen and nitrogen atoms. Hence, the large electronic distribution on the oxygen and nitrogen atoms obviously shows that this region is a reactive centre where the transfer of electrons takes place from these two neighboring high density centers of the concerned ligand to the cadmium and lead ion surfaces. HOMO and LUMO energies, from Table 2, have been examined in order to find the tendency of the studied ligand to donate electrons (to empty molecular orbitals with low energy of convenient molecules), or to accept electrons, respectively.

Table 1. Fukui (f^-) and DFT-based (N_k) indexes of the selected atoms for the Ox^- using NPA population analysis at B3LYP/6-31G(d) level of theory.

Atom k	f^+	f^-	N_k
C1	0.02946	0.17193	1.57422
C2	0.04404	-0.00784	-0.07178
C3	0.02740	0.05504	0.50396
C4	-0.00206	-0.02962	-0.27121
C5	0.02832	0.20778	1.90247
C6	0.05732	-0.02872	-0.26296
C8	0.17939	0.04460	0.40836
C11	0.05828	0.03224	0.29519
C12	0.04720	0.07920	0.72517
O16	0.09103	0.22218	2.03432
N18	0.15918	0.01062	0.09724

The HOMO-LUMO energy gap explains the final charge transfer interaction within the molecule and is useful in determining the electrical transport properties of molecules. A molecule with a high frontier orbital gap (HOMO-LUMO energy gap) has low chemical reactivity and high kinetic stability [46-48]. For example, compounds with a high HOMO-LUMO energy gap are more stable and therefore chemically harder than compounds with a small HOMO-LUMO energy gap [48]. Thus, from Table 2, it can be seen that the oxine compound is soft and less stable, i.e., more reactive, compared to the literature [49]. The electrophilicity index ω indicates whether a molecule tends to exchange electron(s). It is worth noting (see Table 2) that deprotonated oxine molecule has an electrophilicity value of 0.43 eV, which is about twenty times lower than the nucleophilicity (9.16 eV). Theoretically, this reactive ligand can exchange electrons with transition metal ions (acceptors) as a donor. Therefore, the unoccupied *d* orbitals of the metal atom can accept electrons from this molecule (oxine anion) and form a coordinative bond.

Table 2. HOMO and LUMO energies, global reactivity indices μ, η, ω, and N for the deprotonated oxine (Ox^-) compound at B3LYP/6-31G(d) level of theory.

Substrate	E_{HOMO} a.u	E_{LUMO} a.u	μ eV	η eV	ω eV	N eV	Gap eV
Ox^-	0.00138	0.12337	1.70	3.32	0.43	9.16	3.32

In order to see whether the metal chelates with one or two ligands preferably, we have studied the complex of each metal with just one ligand (Ox^-) first.

The complexing reactions of the two studied metals with just one deprotonated oxine are given as:

$$Ox^- + Cd^{2+} \rightleftharpoons [Cd(Ox)]^+ \quad (17)$$

$$Ox^- + Pb^{2+} \rightleftharpoons [Pb(Ox)]^+ \quad (18)$$

The structures of the obtained complexes Cd-oxine (Cd-Ox_1) and Pb-oxine (Pb-Ox_1) are given in Figure 4.

Structurally speaking, both complex structures are planar and almost have a comparable geometry at some extent related to the different formed bonds of the metals with deprotonated oxine.

The HOMO/LUMO for Cd-Ox1 and Pb-Ox1 are presented in Figure 5.

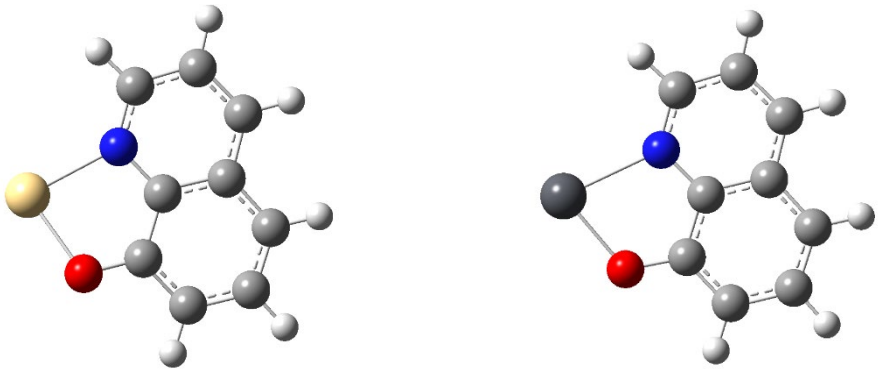

a **b**

Figure 4. Molecular structures of a) Cd-Ox$_1$and b) Pb-Ox$_1$ at B3LYP/6-31G(d).

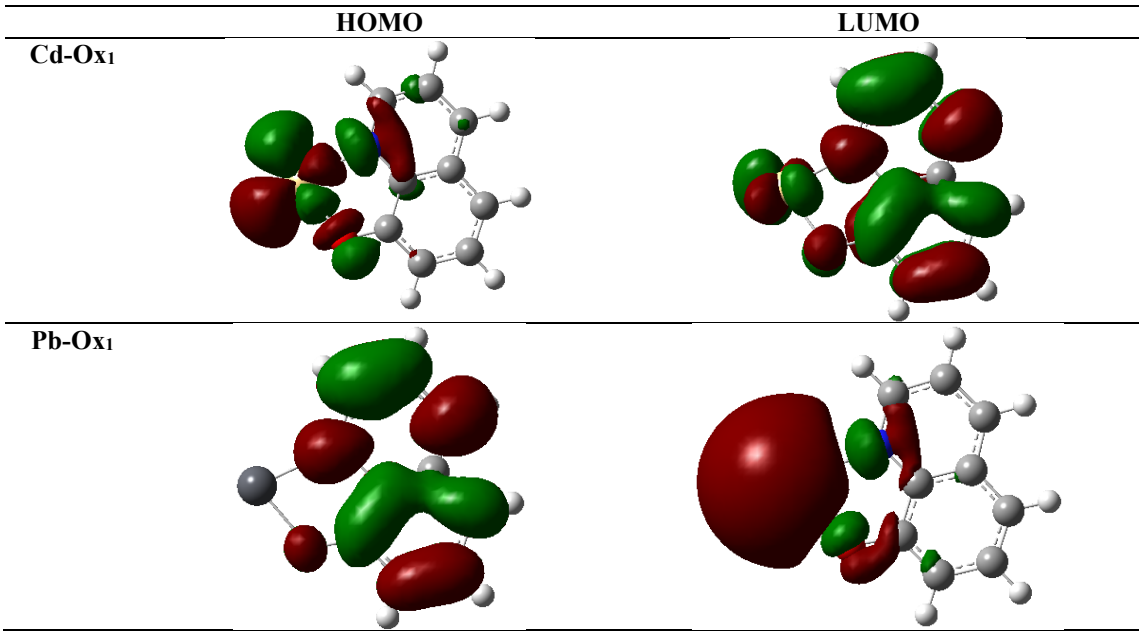

Figure 5. Molecular structures of a) Cd-Ox$_1$ and b) Pb-Ox$_1$ at B3LYP/6-31G(d) for all atoms and B3LYP/SDD for the metal ions.

Table 3. Enthalpy of reaction in the gas and liquid (water) phases for the studied complexes Cd-Ox$_1$ and Pb-Ox$_1$at different levels of theory.

	ΔH_r (kcal/mol)			
Gas	**B3LYP/6-31G(d)**	**B3LYP/cc-pVTZ**	**M06L/6-31G(d)**	**MP2/6-31G(d)**
Cd-Ox$_1$	-372.55	-269.65	-610.50	-251.24
Pb-Ox$_1$	-324.88	-222.23	-532.87	-181.25

	ΔH_r (kcal/mol)			
Water	**B3LYP/6-31G(d)**	**B3LYP/cc-pVTZ**	**M06L/6-31G(d)**	**MP2/6-31G(d)**
Cd-Ox$_1$	-11.08	101.02	-231.05	127.53
Pb-Ox$_1$	-54.61	57.49	-247.15	104.86

Table 4. Entropy of reactionin the gas and liquid phases for the studied complexes at different levels of theory.

			ΔS_r(cal.K^{-1}.mol^{-1})	
Gas	**B3LYP/6-31G(d)**	**B3LYP/cc-pVTZ**	**M06L/6-31G(d)**	**MP2/6-31G(d)**
Cd-Ox$_1$	-30.43	-30.51	-32.98	-30.55
Pb-Ox$_1$	-31.26	-31.34	-33.50	-31.27
			ΔS_r(cal.K^{-1}.mol^{-1})	
Water	**B3LYP/6-31G(d)**	**B3LYP/cc-pVTZ**	**M06L/6-31G(d)**	**MP2/6-31G(d)**
Cd-Ox$_1$	-28.93	-28.91	-31.79	-89.54
Pb-Ox$_1$	-30.36	-30.35	-32.53	-89.54

Table 5. Binding energy in the gas and liquid (water) phases for the studied complexes Cd-Ox$_1$ and Pb-Ox$_1$at different levels of theory.

			ΔG_b(kcal/mol)	
Gas	**B3LYP/6-31G(d)**	**B3LYP/cc-pVTZ**	**M06L/6-31G(d)**	**MP2/6-31G(d)**
Cd-Ox$_1$	-372.55	-260.55	-600.67	-242.13
Pb-Ox$_1$	-324.88	-212.88	-522.88	-171.93
			ΔG_b (kcal/mol)	
Water	**B3LYP/6-31G(d)**	**B3LYP/cc-pVTZ**	**M06L/6-31G(d)**	**MP2/6-31G(d)**
Cd-Ox$_1$	-2.46	109.64	-221.57	137.14
Pb-Ox$_1$	-45.56	66.54	-237.45	114.92

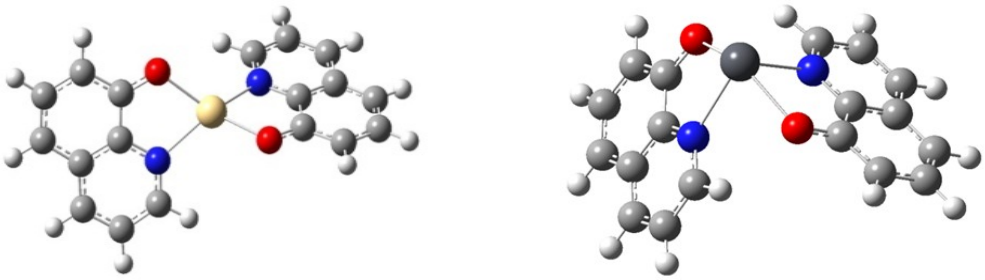

(a) (b)

Figure 6. Molecular structure of the deprotonated oxine complexes with a) Cd^{2+}, and b) Pb^{2+} at the B3LYP/6-31G(d)level of theory.

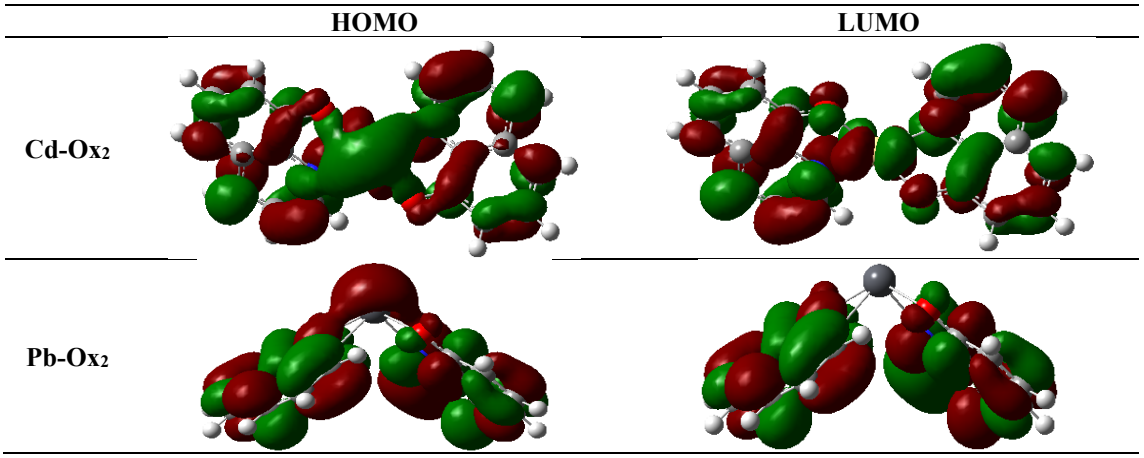

Figure 7. Molecular structures of a) Cd-Ox$_2$ and b) Pb-Ox$_2$ at B3LYP/6-31G(d) for all atoms and B3LYP/SDD for the metal ions.

As presented in Figure 5, the HOMO orbital was located in the cadmium atom orbital while the LUMO was distributed over the oxine ligand for Cd-Ox_1. In contrast, for Pb-Ox_1, the HOMO was distributed over the oxine ligand, and the LUMO orbital was over the lead atom.

In Table 3 are given the complexing reaction enthalpies to explain and understand the thermochemistry of the studied reactions.

As it can be seen from the results shown in Table 3, the reaction enthalpy in the gas phase is negative for both complexes which means that they are exothermic and this for the four theory levels. However, in solvent water only B3LYP/6-31G(d) and M06L/6-31G(d) methods show that the complexing reactions are exothermic. Using the same method B3LYP with a higher basis set (cc-pVTZ) shows that the reactions are endothermic. This discrepancy within the same level simply means that these complexes cannot be at the liquid phase with just one ligand.

The entropy values of the complexing reactions of Cd-Ox_1 and Pb-Ox_1 are listed in Table 4.

The entropy values are negative in both phases meaning that there is a decrease in entropy going from reactants to the complexes. A first look to equations 16 and 17 tells that there is a decreasing of the number of species present from two on the left-hand side to one on the right. Consequently, this leads to a decrease in disorder.

On the other hand, binding free energies are listed in Table 5.

The binding free energies in the gas phase are all negative for both complexes and in all the studied methods. This basically means that these reactions are spontaneous. In addition, the ΔG_b values of Cd-Ox_1 are smaller than the ones corresponding to Pb-Ox_1 showing that Cd-Ox_1 is more stable in the gas phase. However, in water, the ΔG_b values show that these reactions are spontaneous referring to (B3LYP/6-31G(d) and M06L/6-31G(d)) methods. Here, the same thing can be said about B3LYP method as in the gas phase where the results of ΔG_b and spontaneity get inversed after changing just the basis set. Analysing the obtained values show that Pb-$Ox_1$is more stable and that is in all levels of theory which is the contrary of what is found in the gas phase.

Carrying out with the same metals Cd and Pb complexing with two deprotonated oxine ligands this time, the corresponding complexing reactions are given as:

$$2.Ox^- + Cd^{2+} \rightleftharpoons [Cd(Ox)_2] \qquad (19)$$

$$2.Ox^- + Pb^{2+} \rightleftharpoons [Pb(Ox)_2] \qquad (20)$$

The optimised structures are given in Figure 6. It is worthy to note, as it is shown in Figure 6, that the cadmium complex has a twisted tetrahedral geometry and this is in good agreement with experimental literature [50, 51]. Whereas, the lead complex presents a butterfly like geometry. The comparative study of the relative stability of the complexes formed, i.e., cadmium-oxine (Cd-Ox_2) and lead-oxine (Pb-Ox_2), gives a clear idea of the relationship between the detection limit and the stability of the complex in all cases.

The HOMO/LUMO for Cd-Ox2 and Pb-Ox2 are presented in Figure 7.

The HOMO orbital was distributed over the two ligands with a pronounced density on cadmium atom whereas the LUMO was distributed over the ligands and slightly on the cadmium atom. Nevertheless, the HOMO orbital was distributed over the lead atom and the two ligands of oxine while the LUMO was only distributed over the two deprotonated oxine ligands.

In this study, the electrostatic surface ESP maps have been investigated in order to predict the reactive sites in the tested complexes based on locating the positive and negative charged electrostatic potential areas in the complexes (Figure 8).

The reddish color indicates the negative zone corresponding to the minimum electrostatic potential, whereas the bluish color indicates the positive zone with the maximum electrostatic potential. The obtained results show the blue color is concentrated on the region of chelation between the metal ions (Cd^{2+} and Pb^{2+}) with the oxygen and nitrogen atoms of the deprotonated oxine ligand. Both regions are electron-poor zones which mean that are electrophilic. It is worthy to note that the blue part is more pronounced in the Pb-Ox_2 complex. However, the part covering the ligands is green and little bit yellow meaning that are more likely neutral. The thermochemical values (enthalpy) are listed in Table 6.

In the gas phase, the reactions are exothermic since the enthalpy exhibits negative values with the exception of the one obtained with MP2. However, in water, the Pb-Ox_2reaction is exothermic in three levels whereas Cd-Ox_2 complex in just two levels. Here again, the MP2 show that these reactions are endothermic which is not the case since it is proven with more than one method, so it just has to be excluded for this reaction. Moreover, the Pb-Ox2 complexing reaction is more exothermic than Cd-Ox2reaction.

The entropy values of the two complexing reactions are given in Table 7.

Here again, the entropy values for Cd-Ox_2 and Pb-Ox_2 are negative in both phases and that is in all levels of theory. A first glance, it can be seen that

the number of species goes from three on the left-hand side to one on the right in equations 18 and 19 leading to a decrease in disorder.

It is worthy to note that the loss in entropy corresponding to the formation of complexes Cd-Ox_2 and Pb-Ox_2 is bigger about two times than the one corresponding to Cd-Ox_1 and Pb-Ox_1. From equations 17 and 18 to 19 and 20, the complexing reaction is moving from a disordered state to a more ordered one.

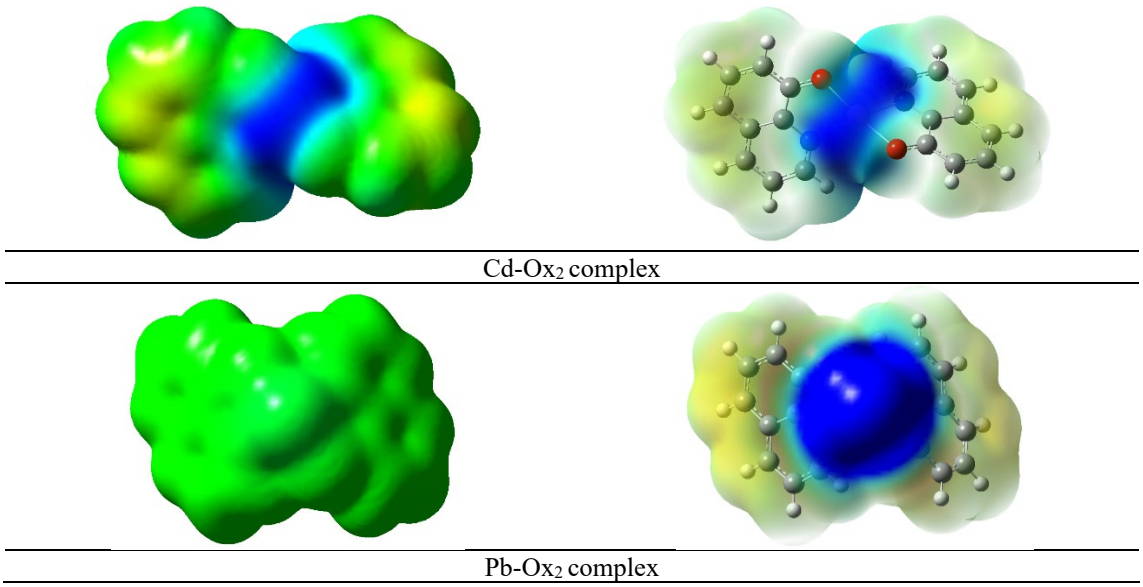

Cd-Ox_2 complex

Pb-Ox_2 complex

Figure 8. ESP maps for the complexes Cd-Ox_2 complex and Pb-Ox_2 complex at B3LYP/SDD method.

Table 6. Enthalpy of reaction in the gas and liquid phases for the studied complexes Cd-Ox_2 and Pb-Ox_2 at different levels of theory.

	ΔH_r (kcal/mol)			
Gas	**B3LYP/6-31G(d)**	**B3LYP/cc-pVTZ**	**M06L/6-31G(d)**	**MP2/6-31G(d)**
Cd-Ox_2	-526.81	-302.85	-729.48	-33.07
Pb-Ox_2	-646.84	-422.88	-615.78	55.41

	ΔH_r (kcal/mol)			
Water	**B3LYP/6-31G(d)**	**B3LYP/cc-pVTZ**	**M06L/6-31G(d)**	**MP2/6-31G(d)**
Cd-Ox_2	-401.13	2.4	-227.05	564.16
Pb-Ox_2	-440.55	-37.0	-254.31	508.61

Table 7. Entropy of reaction in the gas and liquid phases for the studied complexes at different levels of theory.

	ΔS_r(cal.K^{-1}.mol^{-1})			
Gas	**B3LYP/6-31G(d)**	**B3LYP/cc-pVTZ**	**M06L/6-31G(d)**	**MP2/6-31G(d)**
Cd-Ox_2	-73.40	-73.54	-75.57	-67.72
Pb-Ox_2	-74.61	-74.76	-77.60	-71.77

	ΔS_r(cal.K^{-1}.mol^{-1})			
Water	**B3LYP/6-31G(d)**	**B3LYP/cc-pVTZ**	**M06L/6-31G(d)**	**MP2/6-31G(d)**
Cd-Ox_2	-76.94	-74.15	-76.70	-78.46
Pb-Ox_2	-75.20	-72.10	-76.26	-77.13

It is well known that an increase in entropy (disorder) leads to more favorable complexes. However, free energy not only depends on entropy but to the enthalpy too as shown in equation 21.

$$\Delta G = \Delta H - T\Delta S \qquad (21)$$

The enthalpy quantities, in water, for the complexes Cd-Ox_1 and Pb-Ox_1 are smaller than those obtained for Cd-Ox_2 and Pb-Ox_2within the B3LYP/6-31G(d) method. This basically leads to say that Cd-Ox_2 and

Pb-Ox_2 are more exothermic and thus their formation is favorable.

So, these reactions are controlled by the enthalpy factor and not entropy.

The binding free energies of both complexes are listed in Table 8.

The results shown in Table 8 above show that in the gas phase the stability of the complexes is variable depending on the level of theory. For instance, B3LYP at both basis sets shows that the Pb-oxine complex is more stable, whereas M06L and MP2 show that Cd-oxine complex is more stable. This simply is an argument about the uncertainty of the stability of both complexes in the gas phase.

However, as it is given in Table 8, all used methods in this study show that both complexes are stable and that the Pb-oxine complex is more stable than Cd-oxine complex in the liquid phase. This is in good agreement with the experimental findings.

The comparison between the two kinds of the formed complexes Cd-Ox_1, Pb-Ox_1, Cd-Ox_2 and Pb-Ox_2 is quite interesting in terms of stability as shown in Table 9.

Table 8. Binding energy in the gas and liquid phases for the studied complexes Cd-Ox_2 and Pb-Ox_2 at different levels of theory.

	ΔG_b (kcal/mol)			
Gas	**B3LYP/6-31G(d)**	**B3LYP/cc-pVTZ**	**M06L/6-31G(d)**	**MP2/6-31G(d)**
Cd-Ox_2	-505.58	-281.58	-729.48	-12.88
Pb-Ox_2	-624.59	-400.59	-615.78	76.81

	ΔG_b (kcal/mol)			
Water	**B3LYP/6-31G(d)**	**B3LYP/cc-pVTZ**	**M06L/6-31G(d)**	**MP2/6-31G(d)**
Cd-Ox_2	-378.19	24.48	-204.18	521.56
Pb-Ox_2	-418.13	-15.55	-231.57	465.07

Table 9. Energy gaps for the deprotonated oxine (Ox^-) compound, Cd-Ox_1, Pb-Ox_1, Cd-Ox_2 and Pb-Ox_2 at B3LYP/6-31G(d) for all atoms and B3LYP/SDD for the metal ions levels of theory.

Substrate	**Ox^-**	**Cd-Ox_1**	**Pb-Ox_1**	**Cd-Ox_2**	**Pb-Ox_2**
E_{HOMO} (a.u)	0.00138	-0.36155	-0.36478	-0.19795	-0.19254
E_{LUMO} (a.u)	0.12337	-0.31516	-0.25721	-0.07398	-0.06930
E_{Gap}(eV)	3.32	1.26	2.93	3.37	3.35

As it can be seen from Table 9, the reduction of the E_{gap} values after complexation of one deprotonated oxine with the metal ions is assumed to reflect the chemical reactivity and low stability of these complexes. However, the E_{gap} values after complexation of two deprotonated oxines with the metal ions are bigger than the ones corresponding to Cd-Ox_1 and Pb-Ox_1 and free ligand which indicates that the Cd-Ox_2 and Pb-Ox_2 are the most stable complexes. The stability of both complexes Cd-Ox_2 andPb-Ox_2 is almost equivalent and in the same order of magnitude. The detection limit order is 0.17 and 0.45 ppb for cadmium and lead, respectively, when using oxine as ligand [52]. In this study, it has been found in aqueous phase that the stability goes inversely with the detection limit i.e. the most stable complex, Pb-Ox_2, exhibits the highest value of LOD and vice versa for the Cd-Ox_2. This finding is not in good agreement with our previous published papers on the relationship of LOD with respect to the complex stability [27-30]. Experimentally speaking, the stability of coordination compounds in solution means the degree of association between the metal ion and the ligands involved in the state of equilibrium. In metal complexes, there are several factors that can affect the stability, which include: nature of the central metal ion, nature of the ligand, chelating effect, macrocyclic effect, resonance effect, steric effect or steric hindrance. The presence of two donor atoms for complexation means that the chelating effect is present to form stable complexes. The enhanced stability between the two formed complexes is known as the chelate effect variation and is due to the degree of affinity of a ligand for an atom. As it is well stated above, a detection limit (LOD) as an essential parameter in analytical methods, is defined as the lowest quantity or concentration of an analyte in a sample that can be reliably detected with a given analytical method. In our study, using two different metals with oxine as ligand, the response of the system is in direct relation with the metal complex formation. This is why the lowest concentration for Cd and Pb are respectively, 0.17 and 0.45 ppb. Especially with regard to the stability of a metal-oxine complex, the

radius of the metal ion was considered to be one of the most important factors [53]. In our case, the ionic radii of cadmium and lead are 0.78 Å and 0.98 Å, respectively [54]. For metals carrying the same charge, the stability of the complex increases when the ionic radius tends to decrease [55]. The values of binding energy in the gas and liquid phases for both complexes show a greater affinity of oxine for the Pb cation compared to the Cd cation. This shows that the Pb-Ox_2 complex is the most stable. Based on the current theoretical study, results show that the stability of complexes depends on the nature of the central atoms and the ligand [27].This finding can be explained by the fact that when increasing the nuclear charge from Cd to Pb, the binding energy increases due to the enhanced electrostatic interaction between ligand and metal ion which means that high electronic exchange has been established between Pb cations and the deprotonated oxine and more Pb metal cations are being attracted by the ligand.

This paper presents a study dealing with the relationship between the detection limit of trace elements in the AdSV technique and the energetic stability of the complexes formed. For this purpose, some quantum chemical calculations were carried out at the B3LYP, MP2 and M06L theory levels in conjunction with 6-31G(d), cc-pVTZ and SDD basis sets for the deprotonated oxine molecule as a ligand to investigate the structural and electronic properties and to fathom the reactivity and selectivity of the molecular centre. The results show that the deprotonated oxine molecule has a very strong selective centre (oxygen) when bonded with cadmium and lead. The nitrogen atom is less reactive than oxygen, but could be preferred as a target for electrophilic attack of the metals. The negative values of enthalpy in both phases (gaz and solvent) strongly support the exothermic nature of the complexing reactions. The negative values of Gibbs free energy confirm the spontaneous nature and feasibility of the reaction process. The theoretical study at the levels of theory used here shows a greater affinity of the lead metal cations for the deprotonated oxine molecules, which makes it clear that the chemical stability of the lead complex Pb-Ox_2 is greater than that of cadmium one when comparing the binding energy values calculated in both the gas and aqueous phases. According to the DFT calculations, the formation of Cd-Ox_2 and Pb-Ox_2 complexes is more favourable than the other complexes containing only one ligand. This finding is in good agreement with the experimental literature. i.e. Pb cations being more bounded to the ligand gives it higher LOD value. In addition, our results demonstrate that the B3LYP level of theory would be a method of choice for geometry optimization and chemical energy computations of the metal/ligand complexes under study.

Acknowledgments

The author would like to thank the Higher School in Applied Sciences and the University of Abou Bekr Belkaïd for supporting this work.

References

[1] T. Attar, “A mini-review on importance and role of trace elements in the human organism,” Chemical Review Letters, 3 (2020) 117-130.

[2] T. Attar, Y. Harek, N. Dennouni-Medjati, et al., “Dosage du cadmium et du plomb dans le sang humain par voltamétrie à redissolutionanodique,” Annales de Biologie Clinique, 70 (2012) 595-8.

[3] G. Flora, D. Gupta, A. Tiwari, “Toxicity of lead: a review with recent updates,” Interdisciplinary Toxicology, 5 (2012) 47-58.

[4] T. Attar, “Levels of serum copper and zinc in healthy adults from the west of Algeria,” *SPC* Journal of Environmental Sciences, 1 (2019) 26-28.

[5] C.C. Bridges, R.K. Zalups, “Molecular and ionic mimicry and the transport of toxic metals,” Toxicology and Applied Pharmacology, 204 (2005) 274-308.

[6] D. Mohan, K.P. Singh, “Single- and multi-component adsorption of cadmium and zinc using activated carbon derived from bagasse-an agricultural waste,” Water Research, 36 (2020) 2304-2318.

[7] T. Attar, Y. Harek, N. Dennouni-Medjati, et al., “Determination of zinc levels in healthy adults from the west of Algeria by differential pulse anodic stripping voltammetry,” Journal: Journal of Advances in Chemistry, 6 (2013) 855-860.

[8] M. Serge, B.R. Karanga Yssouf, T. Issa, et al., “Electrochemical determination of diuron in soil using a nanocrystalline cellulose modified carbon paste electrode,” International Journal of Electrochemical Science, 16 (2021) 1-15.

[9] N. Thị Hue, N. Van Hop, H. Thai Long, et al., “Determination of chromium in natural water by adsorptive stripping voltammetry using in situ bismuth film electrode,” Journal of Environmental and Public Health, 2020 (2020) 1-10.

[10] H. Evard, A. Kruve, I. Leito, "Tutorial on estimating the limit of detection using LC-MS analysis, part II: Practical aspects," Analytica Chimica Acta, 942 (2016) 40-49.

[11] T. Attar, Y. Harek, L. Lahcen, "Determination of ultra trace levels of copper in whole blood by adsorptive stripping voltammetry," Korean Chemical Society, 57 (2013) 568-573.

[12] T. Attar, Y. Harek, L. Lahcen, "Determination of copper in whole blood by differential pulse adsorptive stripping voltammetry," Mediterranean Journal of Chemistry, 2 (2014) 691-700.

[13] I.H. Taşdemir, M.A. Akay, N. Erk, "Voltammetric behavior of telmisartan and cathodic adsorptive stripping voltammetric method for its assay in pharmaceutical dosage forms and biological fluids," Electroanalysis, 22 (2010) 2101-2109.

[14] P. Leanderson, C. Tagesson, "Iron bound to the lipophilic iron chelator, 8-hydroxyquinoline, causes DNA strand breakage in cultured lung cells" Carcinogenesis, 17 (1996) 545-550.

[15] G. Lescoat, S. Léonce, A. Pierré, et al.,"Antiproliferative and iron chelating efficiency of the new bis-8-hydroxyquinoline benzylaminechelator S1 in hepatocyte cultures," Chemico-biological interactions, 195 (2012) 165-172.

[16] R.B. Dixit, T.S. Patel, S.F. Vanparia, et al.,"DNA-binding interaction studies of microwave assisted synthesized sulfonamide substituted 8-hydroxyquinoline derivatives," Scientia pharmaceutica, 79 (2011) 293-308.

[17] W.Q. Ding, B. Liu, J.L. Vaught, et al., "Anticancer activity of the antibiotic clioquinol," Cancer Research, 65 (2005) 3389-3395.

[18] S. Prachayasittikul, A. Worachartcheewan, R. Pingaew, et al., "Metal complexes of uracil derivatives with cytotoxicity and superoxide scavenging activity," Letters in Drug Design & Discovery, 9 (2012) 282-287.

[19] Y. Anjaneyulu, R.P. Rao, R.Y. Swamy, et al.,"In vitro antimicrobial-activity studies on the mixed ligand complexes of Hg(II) with 8-hydroxyquinoline and salicylic acids," Proceedings of the Indian Academy of Sciences-Chemical Sciences, 91 (1982) 157-163.

[20] C.M. Van Den Berg, "Determination of copper, cadmium and lead in seawater by cathodic stripping voltammetry of complexes with 8-hydroxyquinoline," Journal of Electroanalytical Chemistry and Interfacial Electrochemistry, 215 (1986) 111-121.

[21] H. Darougari, M. Rezaei-Sameti, "The drug delivery appraisal of Cu and Ni decorated B12N12 nanocage for an 8-hydroxyquinoline drug: A DFT and TD-DFT computational study," Asian Journal of Nanoscience and Materials, 5 (2022) 196-210.

[22] A. Cipurković, E. Horozić, S. Marić, et al., "Metal complexes with 8-hydroxyquinoline: synthesis and in vitro antimicrobial activity," Open Journal of Applied Sciences, 11 (2021) 1-10.

[23] V.V.N. Ravi Kishore, A. Aziz, K.L. Narasimhan, et al., "On the assignment of the absorption bands in the optical spectrum of Alq3," Synthetic Metals, 126 (2002) 199-205.

[24] R. Rahier, A. Noiriel, A. Abousalham, "Development of a direct and continuous phospholipase D assay based on the chelation-enhanced fluorescence property of 8-hydroxyquinoline," Analytical chemistry, 88 (2016) 666-674.

[25] J. Murgich, H.J. Franco, "A Density functional theory study of the topology of the charge density of complexes of 8-hydroxyquinoline with Mn(III), Fe(III), and Co(III)," *The Journal of Physical Chemistry A, 113* (**2009**) 5205-5211.

[26] M. Amati, S. Belviso, P.L. Cristinziano, et al., "8-hydroxyquinoline monomer, water adducts, and dimer. Environmental influences on structure, spectroscopic properties, and relative stability of cis and trans conformers," The Journal of Physical Chemistry A, 111 (2007) 13403-13414.

[27] N. Benhadria, T. Attar, B. Messaoudi, "Understanding the link between the detection limit and the energy stability of two quercetin–antimony complexes by means of conceptual DFT," South African Journal of Chemistry, 73 (2020) 120-124.

[28] T. Attar, B. Messaoudi, N. Benhadria, "DFT theoretical study of some thiosemicarbazide derivatives with copper," Chemistry & Chemical Technology, 14 (2020) 20-25.

[29] N. Benhadria, B. Messaoudi, T. Attar, "The study of the correlation between the detection limit and the energy stability of two antimony complexes by means of conceptual DFT," Malaysian Journal of Chemistry, 22 (2020) 111-120.

[30] B. Messaoudi, T. Attar, N. Benhadria, "DFT study of some copper complexes and their detection limits," Chemistry and Chemical Technology, 16 (2022) 185-194.

[31] A. Cipurković, E. Horozić, S. Marić, et al., "Metal complexes with 8-hydroxyquinoline: synthesis and in vitro antimicrobial activity," Open Journal of Applied Sciences, 11 (2021) 1-10.

[32] AD. Becke, "Density-functional thermochemistry. III. The role of exact exchange," The Journal of Chemical Physics, 98 (1993) 5648-5652.

[33] L. Domingo, M. Aurell, P. Perez, et al., "Quantitative characterization of the global electrophilicity power of common diene/dienophile pairs in Diels–Alder reactions," Tetrahedron, 58 (2002) 4417-4423.

[34] J. Tomasi, B. Mennucci, E. Cancès, "The IEF version of the PCM solvation method: An overview of a new method addressed to study molecular solutes at the QM ab initio level," Journal of Moecular Structure (Theochem), 464 (1999) 211-226.

[35] M. Cossi, N. Rega, G. Scalmani, et al., "Energies, structures, and electronic properties of molecules in solution with the C-PCM solvation model," Journal of Computational Chemistry, 24 (2003) 669-681.

[36] J. Tomasi, B. Mennucci, R. Cammi, "Quantum mechanical continuum solvation models," Chemical Review, 105 (2005) 2999-3093.

[37] S. Pokharia, R. Joshi, M. Pokharia, et al., "A density functional theory insight into the structure and reactivity of diphenyltin(IV) derivative of glycylphenylalanine," Main Group Metal Chemistry, 39 (2016) 77-86.

[38] K.A. Moltved, K.P. Kepp, "Using electronegativity and hardness to test density functional," Chemical Physics, 152 (2020) 1-12.

[39] R.G. Parr, L.V. Szentpaly, S. Liu, "Electrophilicity index," Journal of American Chemical Society, 121 (1999) 1922-1924.

[40] A. Benchadli, T. Attar, B. Messaoudi, et al., "Polyvinylpyrrolidone as a corrosion inhibitor for carbon steel in a perchloric acid solution: effect of structural size," Hungarian Journal of Industry and Chemistry, 49 (2021) 59-69.

[41] T. Attar, A. Benchadli, B. Messaoudi, et al., "Experimental and theoretical studies of eosin Y dye as corrosion inhibitors for carbon steel in perchloric acid solution," Bulletin of Chemical Reaction Engineering & Catalysis, 15 (2020) 454-464.

[42] T. Attar, F. Nouali, Z. Kibou, et al., "Corrosion inhibition, adsorption and thermodynamic properties of 2-aminopyridine derivatives on the corrosion of carbon steel in sulfuric acid solution," Journal of Chemical Sciences, 133 (2021) 109-119.

[43] M. Abreu-Quijano, M. Palomar-Pardavé, A. Cuan, "Quantum chemical study of 2-mercaptoimidazole, 2-mercaptobenzimidazole, 2-mercapto-5-methylbenzimidazole and 2-mercapto-5-nitrobenzimidazole as corrosion inhibitors for steel," International Journal of Electrochemical Sciences, 6 (2011) 3729-3742.

[44] H.T. He, X. Lecai, Z. Jingsen, et al., "Binding characteristics of Cd^{2+}, Zn^{2+}, Cu^{2+} and Li^{+} with humic substances: implication to trace element enrichment in low-rank coals," Energy Exploration & Exploitation, 34 (2016) 735-745.

[45] T. Sakajiri, H. Yajima, T. Yamamura, "Density functional theory study on metal-binding energies for human serum transferrin-metal complexes," International Scholarly Research Notices, 2012 (2012) 1-5.

[46] H. Hata, D. Phuoc Tran, M. Marzouk Sobeh, et al., "Binding free energy of protein/ligand complexes calculated using dissociation parallel cascade selection molecular dynamics and Markov state model," Biophys Physicobiology, 18 (2021) 305-316.

[47] J. Aihara, "Reduced HOMO−LUMO gap as an index of kinetic stability for polycyclic aromatic hydrocarbons," Journal of Physical Chemistry A, 103 (1999) 7487-7495.

[48] D.E. Manolopoulos, J.C. May, S.E. Down, "Theoretical studies of the fullerenes: C34 to C70," Chemical Physics Letters, 181 (1991) 105-111.

[49] Y. Ruiz-Morales, "HOMO−LUMO gap as an index of molecular size and structure for polycyclic aromatic hydrocarbons (PAHS) and asphaltenes: a theoretical study,"Journal of Physical Chemistry A, 106 (2002) 11283-11308.

[50] A. Asghar, M.M. Bello, A.A.A. Raman, et al., "Predicting the degradation potential of Aacid blue 113 by different oxidants using quantum chemical analysis," Heliyon, 5 (2019) e02396.

[51] M. Dudev, J. Wang, T. Dudev, et al., "Factors governing the metal coordination number in metal complexes from cambridge structural database analyses," The Journal of Physical Chemistry B, 110 (2006) 1889-1895.

[52] G. Kuppuraj, M. Dudev, C. Lim, "Factors governing metal−ligand distances and coordination geometries of metal complexes," The Journal of Physical Chemistry B, 113 (2009) 2952-2960.

[53] N.M. Thanh, N.D. Luyen, T. Thanh Tam Toan, et al., "Voltammetry determination of Pb(II), Cd(II), and Zn(II) at bismuth film electrode combined with 8-hydroxyquinoline as a complexing agent," Journal of Analytical Methods in Chemistry, 2019 (2019) 1-11.

[54] T. Yamamura, K. Ichimura, T. Tsuda, et al., "Lanthanoid complex of iron-transport protein, transferring-kinetic-study on release of the metal from N-binding and C-binding sites," Nippon Kagaku Kaishi, 4 (1988) 452-458.

[55] R.D. Shannon, "Revised effective ionic radii and systematic studies of interatomic distances in halides and chalcogenides," Acta crystallographica section A: crystal physics, diffraction, theoretical and general crystallography, 32 (1976) 751-767.

[56] T. Rakitskaya, A. Truba, E. Radchenko, et al., "Mono- and bimetallic complexes of Mn(II), Co(II), Cu(II), and Zn(II) with schiff bases immobilized on nanosilica as catalysts in ozone decomposition reaction," Chemistry and Chemical Technology, 12 (2018) 1-6.